Structure and Magnetism of Ce_5Pb_3O

Robin T. Macaluso,[†] N. O. Moreno,[‡] Z. Fisk,[§] J. D. Thompson,[‡] and Julia Y. Chan*,[†]

Department of Chemistry, Louisiana State University, Baton Rouge, Louisiana 70803, MST-10, Los Alamos National Laboratory, Los Alamos, New Mexico 87454, and NHMFL, Florida State University, Tallahassee, Florida 32306

Received December 2, 2003. Revised Manuscript Received February 17, 2004

Single crystals of Ce_5Pb_3O have been synthesized by flux growth. This compound adopts the tetragonal *I*4/*mcm* space group with lattice parameters of $a = b = 8.5870(2)$ Å and $c = 14.3870(5)$ Å, $Z = 4$. The crystal structure of Ce_5Pb_3O consists of a network of interpenetrating corner-sharing Ce-centered Pb_6 octahedra and O-centered Ce_4 tetrahedra. The tetrahedra are linked to each other by Pb trigonal antiprisms. Magnetization measurements show that Ce_5Pb_3O orders ferrimagnetically at $T_c = 46$ K, the second-highest known ordering temperature for any Ce-based intermetallic compound.

Introduction

Cerium intermetallics exhibit a wide variety of interesting ground states, ranging from magnetically ordered and superconducting with unconventional pairing to valence fluctuating and "Kondo insulator" behavior. Crystal structures in which these materials form can influence the ground state configuration. Of those Ce-based compounds that order magnetically, the vast majority order antiferromagnetically, with almost all of these ordering below 10 K. Unlike the antiferromagnets, only a dozen or so Ce compounds order ferromagnetically. This rare class of materials includes several ternary Ce−T−X compounds where T = transition metal and X = main-group element. Some examples include CeAuGe,[1] $CeRu_2Ge_2$,[2] $CeRhSn_2$,[3] CePdSb,[4] $CeNiIn_2$,[5] and $CeAgSb_2$,[6,7] which possess ordering temperatures ranging between 3.4 and 10 K. A notable exception is the boride compound $CeRh_3B_2$, which orders ferromagnetically at $T_c = 115$ K, which is by far the highest ordering temperature of any Ce compound to date.[8] Unlike the Ce−T−X compounds previously mentioned, the magnetism in $CeRh_3B_2$ is not due to the 4f electron of Ce. Instead, an anomalous unit cell volume indicates that Ce is in a mixed 3+/4+ state, and the authors suggest that it is the 4d electrons of Rh that mediate the ferromagnetic properties. Another possible exception is CeScGe, in which Ce moments may order ferromagnetically at 46 K;[9] although some experiments suggest that this transition is due to the antiferromagnetic state.[10]

In our search for novel Ce-containing intermetallic compounds, we have discovered Ce_5Pb_3O. Magnetic measurements reveal that this compound orders ferrimagnetically below $T_c = 46$ K, which to the best of our knowledge is the second-highest ordering temperature for any Ce-containing compound.

Experimental Section

Synthesis. Ce_5Pb_3O was synthesized by the flux growth method. Our original intent was to grow single crystals of a ternary compound containing Ce, Co, and Pb. Ce (99.999%, Ames Laboratory), Co (99.998%, Alfa Aesar), and Pb (99.9999%, Alfa Aesar) were placed in an alumina crucible with a ratio of 7:2:1. The crucible and it contents were then sealed into an evacuated quartz tube and heated in a furnace at 1175 °C for 4 h. After cooling to 850 °C, the tube was removed from the furnace, inverted, and centrifuged. Large black rectangular crystals were mechanically separated from the crucible. Typical crystal size was approximately $8 \times 0.5 \times 0.6$ mm^3.

It is of interest to note that although Co was included in the initial mixture, no Co was found in the single crystals. Flux growth using 5 mol of Ce:3 mol of Pb or 5 mol of Ce:20 mol of Pb and the same temperature profile as described above fails to yield Ce_5Pb_3O, at least in significant amounts according to X-ray powder diffraction. In addition, the synthesis procedure with the inclusion of Co has been performed on several occasions, and single crystals of Ce_5Pb_3O are obtained each time.

X-ray Diffraction. Fragments of the crystals obtained from the reaction described above were mounted onto the goniometer of a Nonius Kappa CCD diffractometer equipped with Mo Kα radiation ($\lambda = 0.71073$ Å). Data were collected up to $\theta =$

* To whom correspondence should be addressed. Telephone: (225) 578-2695. Fax: (225) 578-3458. E-mail: jchan@lsu.edu.
† Louisiana State University.
‡ Los Alamos National Laboratory.
§ Florida State University.

(1) Pöttgen, R.; Borrmann, H.; Kremer, R. K. *J. Magn. Magn. Mater.* **1996**, *152*, 196.
(2) Besnus, M. J.; Essaihi, A.; Hamdaoui, N.; Fischer, G.; Kappler, J. P.; Meyer, A.; Pierre, J.; Haen, P.; Lejay, P. *Physica B* **1991**, *171*, 350.
(3) Hossain, Z.; Gupta, L. C.; Geibel, C. *J. Phys.: Condens. Matter* **2002**, *115*, 9687.
(4) Malik, S. K.; Adroja, D. T. *Phys. Rev. B* **1991**, *43*, 6295.
(5) Zaremba, V.; Kalychak, Y. M.; Tyvanchuck, Y. B.; Hoffmann, R.-D.; Moller, M. H.; Pöttgen, R. *Z. Naturforsch.* **2002**, *57b*, 791.
(6) Sologub, O.; Nöel, H.; Leithe-Jasper, A.; Rogl, P.; Bodak, O. I. *J. Solid State Chem.* **1995**, *115*, 441.
(7) Sidorov, V. A.; Bauer, E. D.; Frederick, N. A.; Jeffries, J. R.; Nakatsuji, S.; Moreno, N. O.; Thompson, J. D.; Maple, M. B.; Fisk, Z. *Phys. Rev. B* **2003**, *67*, 224419.
(8) Khar, S. K.; Malik, S. K.; Vijayaraghavem, R. *J. Phys. C: Solid State Phys.* **1981**, *14*, L321.
(9) Canfield, P. C.; Thompson, J. D.; Fisk, Z. *J. Appl. Phys.* **1991**, *70*, 5992.
(10) Singh, S.; Dhar, S. K.; Mitra, C.; Paulose, P.; Manfrinetti, P.; Palenzona, A. *J. Phys.*: *Condens. Matter* **2001**, *12*, 3753.

10.1021/cm0352605 CCC: $27.50
Published on Web 03/23/2004

Table 1. Crystallographic Parameters

Crystal Data	
formula	Ce_5Pb_3O
a (Å)	8.5870(2)
c (Å)	14.3870(5)
V (Å^3)	1060.85(5)
Z	4
crystal dimension (mm^3)	0.03 × 0.05 × 0.08
temperature (°C)	25
crystal system	tetragonal
space group	$I4/mcm$
θ range (deg)	2.55−30.03
μ (mm^{-1})	68.335
Data Collection	
measured reflections	1296
independent reflections	446
reflections with $I > 2\sigma(I)$	431
R_{int}	0.0346
h	−12 → 12
k	−8 → 8
l	−20 → 16
Refinement	
R1[$F^2 > 2\sigma(F^2)$]	0.0301
wR(F^2)	0.1034
reflections	446
parameters	17
$\Delta\rho_{max}$ (e Å^{-3})	3.007
$\Delta\rho_{min}$ (e Å^{-3})	−3.143
extinction coefficient	0.00044(9)
T_{min}, T_{max}	0.023, 0.129

[a] $R1 = \Sigma||F_o| - |F_c||/\Sigma|F_o|$. [b] $wR2 = \Sigma[w(F_o^2 - F_c^2)]/\Sigma[w(F_o^2)^2]^{1/2}$.

Table 2. Atomic Positions and Displacement Parameters of Ce_5Pb_3O

atom		x	y	z	U_{eq}[a] (Å^2)
Ce1	4c	0	0	0	0.0181(4)
Ce2	16l	0.65306(5)	0.15306(5)	0.15052(6)	0.0120(3)
Pb1	4a	0	0	1/4	0.0126(3)
Pb2	8h	0.85631(5)	0.35631(5)	0	0.0114(3)
O	4b	1/2	0	1/4	0.014(3)

[a] U_{eq} is defined as one-third of the trace of the orthogonalized $\mathbf{U}_{ij}$ tensor.

30° at 293 K. Further crystallographic parameters are provided in Table 1. The structural model was initially determined from a direct methods solution using SHELXS-97 and refined using SHELXL97.[11] Because the lattice parameters were very similar to those of La_5Pb_3O,[12] the structure was refined using La_5Pb_3O as an initial structural model. After refinement with isotropic displacement parameters, an electron density peak of ∼11 e/Å^3 was found at the 4b site, indicating the presence of a small atom. Refining the data with partial occupancy of Co on the 4b site led to a poor structural model with the isotropic displacement parameter, U_{iso}, being too large (U_{iso} = 0.354); however, refinement of the data with O on the 4b site resulted in R1 = 3.36%. Refining the anisotropic displacement parameters and extinction led to R1 = 3.01%. All of the anisotropic displacement parameters were well-behaved except for that of the Ce1 atom located at the 4c site. The U_{33} (= 0.0351(9)) of Ce1 was larger than $U_{11} = U_{22}$ (= 0.0097(4)) by a factor of 3.6. Additional diffraction experiments on several fragments from different synthesis attempts are in agreement.

Cobalt was not detected with EDX analysis. Atomic positions and displacement parameters are provided in Table 2, and selected interatomic distances and bond angles are given in Table 3.

Physical Property Measurements. Magnetic measurements were made using a Quantum Design SQUID (*S*uperconducting *Qu*antum *I*nterference *D*evice) magnetometer by zero-field cooling the sample to 5 K and then either sweeping the temperature with a fixed magnetic field of 1 kOe or sweeping field at constant temperatures of 5 and 30 K. For these measurements, the crystal was mounted on a weakly diamagnetic holder whose magnetic contribution, determined independently, was subtracted to obtain the sample response. This sample holder allowed the crystallographic *c*-axis of the sample to be aligned parallel or perpendicular to the applied magnetic field to within approximately ±5°.

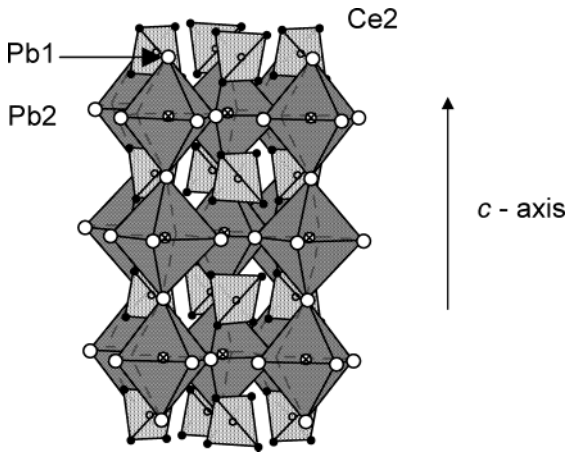

Figure 1. Crystal structure of Ce_5Pb_3O along the *c*-axis is presented. The Ce octahedra are shaded in dark gray with the Pb1 and Pb2 atoms shown as white circles at the vertexes of the octahedron. The O atoms are at the center of the light gray tetrahedra with 4 Ce2 atoms (black circles) at the corners.

Table 3. Select Interatomic Distances (Å) and Bond Angles (deg) for Ce_5Pb_3O

In $CePb_6$ Octahedra			
Ce1−Pb2 (×4)	3.2991(2)	Pb2−Ce1−Pb2	90.0
Ce1−Pb1 (×2)	3.59675(13)	Pb1−Ce1−Pb1	180.0
In Ce_4 Tetrahedra			
O−Ce2 (×4)	2.3459(8)	Ce2−O−Ce2	104.80(4)
Ce2−Ce2 (×4)	3.8864(15)		111.85(2)
Ce2−Ce2 (×2)	3.7174(13)		
Between Ce_4 Tetrahedra			
Ce2−Pb1 (×2)	3.5569(4)	Pb2−Ce2−Pb2	89.47(2)
Ce2−Pb2 (×3)	3.3449(8)	Pb1−Ce2−Pb2	89.952(10)
Ce2−Ce1 (×4)	3.9105(5)	Pb1−Ce2−Pb2	90.949(13)
Pb2 Trigonal Antiprism			
Pb2−Ce2 (×4)	3.2837(9)	Pb1−Ce2−O	90.956
Pb2−Ce2 (×2)	3.3449(8)	Ce2−Pb2−Ce2	88.01(2)

Results and Discussion

Crystal Structure. The structure of Ce_5Pb_3O is shown in Figure 1. The isostructural La_5Pb_3O was first discovered as an impurity in the synthesis of La_5Pb_3Mn.[12] Ce_5Pb_3O crystallizes in the tetragonal $I4/mcm$ space group with Ce1, Ce2, Pb1, and Pb2 occupying the 4c, 16l, 4a, and 8h sites, respectively, and oxygen occupies the interstitial 4b site. Lattice parameters have been determined to be $a = b = 8.5870(2)$ Å and $c = 14.3870(5)$ Å. Ce_5Pb_3O is an interstitial derivative of Ce_5Pb_3, which forms in the hexagonal Mn_5Si_3 structure type.[13] Other compounds such as La_5Ge_3,[14] La_5Pb_3,[15,16] and Zr_5Sb_3[16] have also been shown to host a wide range of interstitial atoms, such as N, O, P, and Zn.

(11) Sheldrick, G. M. *SHELXL97*; University of Göttingen: Göttingen, Germany, 1997.
(12) Guloy, A. M.; Corbett, J. D. *Z. Anorg. Allg. Chem.* **1992**, *616*, 61.
(13) Aronsonn, B. *Acta Chem. Scand.* **1960**, *14*, 1414.
(14) Guloy, A. M.; Corbett, J. D. *Inorg. Chem.* **1993**, *32*, 3532.
(15) Guloy, A.; Corbett, J. D. *J. Solid State Chem.* **1994**, *109*, 352.
(16) Corbett, J. D.; Garcia, E.; Kwon, Y.-U.; Guloy, A. *Pure Appl. Chem.* **1990**, *62*, 103.

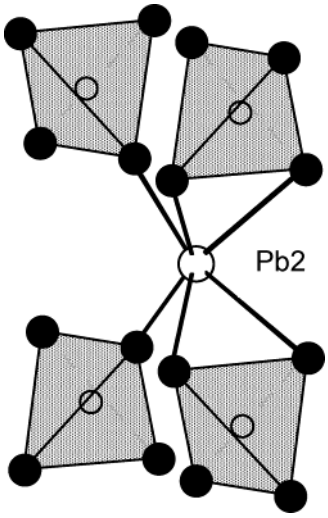

Figure 2. The Pb2 atom links the vertexes of four Ce_4 tetrahedra. Pb is shown as a white circle and Ce2 atoms are shown as black circles. Each tetrahedron shaded in light gray houses an interstitial O atom.

Ce_5Pb_3O can be viewed as a network of interpenetrating Ce-centered Pb_6 octahedra and O-centered Ce_4 tetrahedra. Pb1 and Pb2 occupy the apex and equatorial positions, respectively, of the octahedra. The octahedra are staggered by 45° along the [001] direction. The Ce1−Pb1 and Ce1−Pb2 interatomic distances are 3.59675(13) and 3.2991(2) Å, respectively, resulting in octahedra that are elongated along the *c*-axis. These Ce1−Pb1 interatomic distances are similar to the Ce−Pb interatomic distances of 3.1546−3.5101 Å found in Ce_3Pb[17] and Ce_5Pb_3.[18]

One interesting feature of Ce_5Pb_3O is the ratio of the displacement parameters for Ce1, $U_{33}/U_{11} \sim 3.6$. This has also been observed for La_5Pb_3O, where the displacement parameters are attributed to a split 8f La site with ~50% occupancy on each of the positions.[12] However, refining the *z*-position of Ce1 with the same model resulted in $z = 0.00047 \pm 0.08537$, leading us to conclude that the single-crystal diffraction data could not be resolved sufficiently to differentiate between a model with a split Ce1 site and a model with Ce1 at the origin. Although we cannot conclude with absolute certainty that the Ce site is disordered, the large U_{33} observed in Ce_5Pb_3O suggests disorder, as was found for the analogous La site in La_5Pb_3O.

A view of the Ce_4 tetrahedra is provided in Figure 2. An O atom occupies the center of the tetrahedron with distances of 2.3459(8) Å to 4 Ce2 atoms and Ce2−O−Ce2 bond angles range between 104.81(4)° and 111.85(2)°. This bond distance is in agreement with the calculated radii sum of 2.39 Å[19] and is similar to the La−O distance of 2.3667(7) Å found in La_5Pb_3O.[12] The Pb2 atoms, which occupy the equatorial position of the $CePb_6$ octahedra, also form trigonal antiprisms comprised of Ce2−Pb2 interatomic distances ranging between 3.3450(8) and 3.4895(11) Å. Thus, the O-centered Ce_4 tetrahedra are linked to each other by Pb2 trigonal antiprisms.

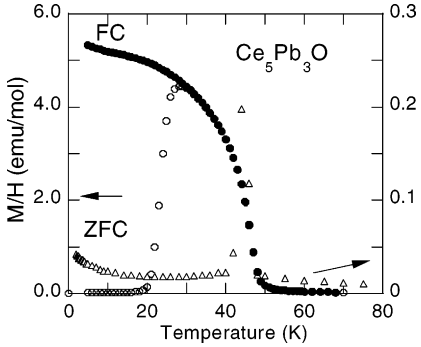

Figure 3. Magnetic susceptibility of Ce_5Pb_3O with $H = 1$ kOe is shown. The open circles correspond to ZFC data and filled circles correspond to FC data. Left scale is asocciated to the H // *ab* plane. Open triangles represent data for the right scale for H // along the *c*-axis.

Magnetic Properties. A plot of the dc magnetic susceptibility, χ, as a function of temperature with applied field, H, of 1 kOe along both the *ab*-plane and *c*-axis is provided in Figure 3. A sudden increase of χ_{ab} below 46 K indicates the onset of magnetic order of the Ce moments, with the *ab*-plane being the easy magnetization direction. Zero-field cooled (ZFC) and field-cooled (FC) magnetic susceptibility along the *ab*-plane show a strong irreversibility at ~29 K. At 29 K, the ZFC curve decreases with temperature until 16 K, where χ reaches a constant value of 0.03 emu/mol, whereas the FC susceptibility increases as the temperature decreases. The transition at 46 K is observed only when the crystallographic *c*-axis is perpendicular to H.

Above 150 K both χ_{ab} and χ_c follow the same Curie−Weiss law ($\chi = \chi_o + C/(T - \theta)$) with a paramagnetic Weiss temperature of $\theta = -12.4(2)$ K, indicative of weak antiferromagnetic correlations, and an effective magnetic moment of $\mu_{eff} = 2.54\ \mu_B$/Ce that is expected for a free trivalent Ce ion. Below 150 K the *ab*-plane susceptibility is enhanced significantly relative to an extrapolation of the higher temperature Curie−Weiss behavior, indicating a dominance of ferromagnetic correlations as well as the influence of crystalline electrical fields on the 4f moment of the Ce^{3+} ion.

Low-field ZFC and FC susceptibility measurements are often used to study spin-glass or spin-glass-like phases. However, for systems where *long-range order* is involved, the contribution can arise from domains, domain walls, and disorder. In local canted spin systems, the ZFC−FC branching behavior has been interpreted in terms of domains; that is, cooling in the presence of an external field helps the domains to grow.[20]

In soft ferromagnetic materials, the magnetization process is composed of two distinct mechanisms.[21] (i) When the field is increased from the saturated region, domains nucleate in the sample, usually starting from the boundaries. (ii) In the central part of the hysteresis loop near the coercive field, the magnetization process is due mainly to domain wall motion. Therefore, at applied magnetic fields much lower than the coercive field, the initial susceptibility of a ferromagnet mono-

(17) Jeitschko, W.; Nowotny, H.; Benesovsky, F. *Monatsh. Chem.* **1964**, *65*, 1040.
(18) Jeitschko, W.; Parthé, E. *Acta Crystallogr.* **1965**, *19*, 275.
(19) Shannon, R. D. *Acta Crystallogr.* **1976**, *A 32*, 751.
(20) Dorman, J. L.; Nogues, M. *J. Phys.*: *Condens. Matter* **1990**, *2*.
(21) Herpin, A. *Théorie du Magnétisme*; Presses Universitaires de France: Paris, 1968.

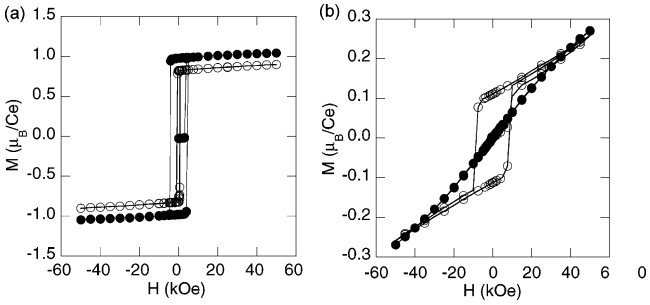

Figure 4. Magnetization of Ce_5Pb_3O as a function of field with the H // ab-plane is shown in (a) and with H // c-axis in (b). The filled circles represent data at $T = 5$ K, and open circles are for $T = 30$ K. The lines are an aid for the eye.

tonically increases with temperature, passing through a maximum below T_c.

Figures 4a and 4b show the hysteresis loops of Ce_5Pb_3O at 5 and 30 K with H parallel to the ab-plane and c-axis, respectively. For H // ab-plane, the saturated magnetic moment is 1.05 μ_B/Ce ion at 5 K, which is smaller than the Ce^{3+} free-ion moment value of 2.14 μ_B/Ce. For the same orientation at 30 K, the saturated moment is 0.9 μ_B, as expected for a transition temperature of 46 K. Saturation moments in the range of 1 μ_B/Ce atom are frequently observed for cerium intermetallics.[1,4]

These small values of the saturated moment are due to crystal electrical field splitting effects on the $J = {}^5/_2$ ground state of the Ce^{3+} ion. The magnetic behavior along the c-axis varies between 5 and 30 K, as can be seen in Figure 4b. The linear behavior at 5 K in the M vs H plot is typical of antiferromagnetic ordering. However, at 30 K, magnetic hysteresis is observed for $H \leq \pm 15$ kOe, above which the magnetization increases with a slope only slightly smaller than is found at 5 K.

These observations suggest that the 46 K transition is due to a paramagnetic to ferrimagnetic transition, whereas the transition at 26 K is ambiguous. In the absence of other measurements, it is not possible to determine if all of the Ce moments are involved in the transition at 46 K. This leaves open the possibility that only some of the Ce moments order at 46 K and others at inequivalent sites order as well at 26 K or that the 26 K transition could be the result of spin reorientation or a 2D transition. Irrespective of the nature of this transition, it as well as the high ordering temperature at the ferrimagnetic transition must be controlled by the particular crystal structure adopted by Ce_5Pb_3O. The nearest neighbor Ce−Ce distance in Ce_5Pb_3O is 3.7174 Å in O tetrahedra, which is greater than 3.25−3.4 Å, the Hill limit beyond which direct 4f−4f interaction ceases.[22] Therefore, the direct f−f interaction can be ruled out as being responsible for the high magnetic ordering temperature of Ce_5Pb_3O.

Acknowledgment. J.Y.C. acknowledges NSF-Career (DMR-0237664) and Alfred P. Sloan Foundation for partial support of this work. R.T.M. acknowledges the GIAR from National Academy of Sciences, administered by Sigma Xi, for partial support. We also thank Dr. Frank Fronczek for useful discussion. Work at LANL was performed under the auspicious of the U.S. Department of Energy. Z.F. gratefully acknowledges support at Florida State University from NSF DMR-0203214 and MST-10 at Los Alamos National Laboratory.

Supporting Information Available: Crystallographic data in CIF format are available for Ce_5Pb_3O. This material is available free of charge via the Internet at http://pubs.acs.org.

CM0352605

(22) Hill, H. H. *Plutonium and Other Actinides*, 2nd ed.; Miner, W. N., Ed.; Metallurgical Society of the AIME: New York, 1970.